Advanced Materials Research Vols. 287-290 (2011) pp 2094-2101
Online available since 2011/Jul/04 at www.scientific.net

doi:10.4028/www.scientific.net/AMR.287-290.2094

Synthesis of mesoporous Zr-P-Al materials with high BET specific surface area without calcination

Ziyu Liu [1,2],Yue Qi [1], Yingxu Wei [1], Zongbin Wu [1] and Zhongmin Liu [1,*]

[1] Dalian Institute of Chemical Physics, CAS, Dalian, Liaoning, 116023, China

[2] Shanghai Advanced Research Institute, CAS, Shanghai, 201203, China

zml@dicp.ac.cn

Keywords: Mesoporous Zr-P-Al material, post-synthetic treatment, high BET specific surface area.

Abstract. A mesostructured zirconium oxide was synthesized hydrothermally using cetyltrimethylammonium bromide (CTAB) as the structure-directing agent and $ZrSO_4.4H_2O$ as the reactant. Subsequent post-synthetic treatment with H_3PO_4 followed by the treatment with $AlCl_3$ solutions resulted in mesoporous Zr-P-Al materials, which exhibited high BET specific surface area before calcination. The phosphoric acid concentration affected the textual data of the resulting Zr-P and Zr-P-Al materials greatly. 0.1-0.5 M H_3PO_4 increased obviously the long-range order of the as-synthesized Zr-P materials while 0.76 M H_3PO_4 decreased it. After calcination at 773 K, the Zr-P materials turned to nonporous materials except the one synthesized by 0.5 M H_3PO_4, which showed micropores with a BET specific surface area of 147 m^2/g. Further treating the Zr-P materials (synthesized from different concentration of phosphoric acid) with the same amount of $AlCl_3$ solution resulted in mesoporous Zr-P-Al materials, but the long-range order of which decreased when the H_3PO_4 concentration increased. Similarly, the BET specific surface area of the above-mentioned Zr-P-Al materials decreased from 462 m^2/g for 0.25 M H_3PO_4 to 394 m^2/g for 0.5 M H_3PO_4 and finally to 332 m^2/g for 0.76 M H_3PO_4 after calcination at 773 K, while the pore size increased gradually from 3.0 to 3.5 nm. It was found that about 90% of the CTAB had been removed during the $AlCl_3$ treatment and that the as-synthesized Zr-P-Al materials exhibited high BET specific surface area as well as mesopores. The $AlCl_3$ amount is another factor affecting the textual data of the uncalcined Zr-P-Al materials besides the H_3PO_4 concentration. With the phosphoric acid concentration of 0.25 M, the BET specific surface area of the as-synthesized Zr-P-Al materials increased from 477 m^2/g to as high as 734 m^2/g with the increasing $AlCl_3$ amount before it decreased from then on.

Introduction

Materials with high BET specific surface area are very attractive for catalytic reactions since they allow a high concentration of active sites or highly dispersed active centers per mass of materials [1-4]. Many efforts have been devoted to increasing the BET specific surface area of materials, among which preparing mesoporous materials is often used. The synthesis of mesoporous materials with extremely high BET specific surface areas of more than 1000 m^2/g was first reported in 1992 through a novel liquid crystal templating method [5,6], which was soon proved to be a useful way to increase the BET specific surface areas of materials. Following this route many mesoporous transition-metal oxides were also synthesized, but these materials usually showed much lower BET specific surface areas compared with the siliceous ones [7-11]. This is caused by the fact that the density of the oxide wall enters the calculation of BET specific surface areas. For the same structural parameter, a wall density which is by a factor of 2 higher results in half of the BET specific surface area. Assuming identical oxide densities as in the crystalline bulk, 1000 m^2/g for silica (density of quartz is 2.6 g/cm^3) corresponds to 605 m^2/g for titania (density of rutile is 4.3 g/cm^3) and 440 m^2/g for zirconia (density of zirconia (baddeleyite) equals to 5.9 g/cm^3) [12]. So decreasing the density of the oxide wall will be an effective way to increase the BET specific surface area of non-siliceous

mesoporous materials. As far as the mesoporous zirconia is concerned, adding other "light" elements during the synthesis may decrease the oxide wall density and therefore increase its BET specific surface area. Aluminum is one of such "light" elements that often used in preparing molecular sieves, if it can be induced to the framework of mesoporous zirconia, its smaller density (3.9 g/cm^3 for α-Al_2O_3) may lead to higher BET specific surface area.

In previous studies [13,14], we have reported the synthesis of mesoporous Zr-P-Al materials by a three-step method, in which a hexagonal zirconium oxide-sulfate composite was prepared and subsequently treated with a phosphoric acid solution followed by the treatment with $AlCl_3$ solutions. With the H_3PO_4 concentration fixed to 0.25 M, adjusting the $AlCl_3$ amount resulted in mesoporous Zr-P-Al materials with BET specific surface area of 314-462 m^2/g after calcination at 773 K. It is easy to wonder if the H_3PO_4 concentration also affects the textual data of the Zr-P-Al materials. In another aspect, we found that part of structure-directing agent had been removed when the Zr-P materials was post-synthetic treated with $AlCl_3$ solutions, so is it possible to obtain porous Zr-P-Al materials without calcination? If this could be achieved, it will simplify the synthesis process and lower the cost of mesoporous materials, which is valuable in applying such materials.

We report here the synthesis of mesoporous Zr-P-Al materials with high BET specific surface area, in which no calcination is necessarily needed. The effect of the H_3PO_4 concentration on the long-range order and textual data of the Zr-P-Al is investigated in detail. How the Al amount affects the BET specific surface area of the as-synthesized Zr-P-Al materials is also discussed.

Experimental

Synthesis. The synthesis procedure is similar to that described before [13,14]. A mixture of CTAB and $Zr(SO_4)_2 \cdot 4H_2O$ was dispersed in deionized water with a molar composition of $Zr(SO_4)_2$: CTAB : H_2O=1: 0.27: 240. After being stirred at 353 K for 2 h, the resulting suspension was crystallized at 373 K for 48 h. The precipitate was centrifuged, washed with deionized water and dried at 373 K. The resulting sample was designated as MZ. Subsequently, 5 g of MZ was stirred, respectively, in 100 ml of phosphoric acid solution with different concentration for 2 h at room temperature. The samples were recovered after being centrifuged and dried, and were designated as MZP_x (x denotes the molar concentration of phosphoric acid). 1 g of MZP_x was stirred in 100 ml of 0.1 M ethylamine solution at ambient temperature for 24 h, then different volume of 0.2 M $AlCl_3 \cdot 6H_2O$ solutions were added to the suspension, and finally, 0.2 M NaOH was slowly dropped in until pH=4.2. These mixtures were refluxed at 368 K for 24 h, then the solids were separated, washed and dried to form the Zr-P-Al materials, which were named as MZP_xAl_y (y=0.7-29), where y is the mass ratio of $AlCl_3 \cdot 6H_2O$ to MZP_x. Calcinations were carried out in air at 773 K for 6 h if necessary, and the compound expression "as-synthesized" is used to refer to the samples without calcination.

Characterization. Powder X-ray diffraction (XRD) patterns were recorded on a D/Max-b X-ray diffractometer with Cu Kα radiation. Fourier transform infrared spectroscopy (FTIR) studies were performed on a Bruker EQUINOX 55 spectrometer by KBr pellet method. The textural data were obtained by nitrogen adsorption measurement using a Micromeritics 2010 BET analyzer. Prior to the measurements, the samples were outgassed at 623 K for at least 4 h.The specific surface area was calculated by the BET method. The pore size distributions were calculated from desorption branches of nitrogenisotherms using the BJH model. Thermogravimetric analysis (TGA) results were obtained on a Perkin-Elmer Pyris 1 thermogravimetric analyzer and differential thermal analysis (DTA) on a Perkin-Elmer DTA 7 differential thermal analyzer, both in air and at a heating rate of 10 K/min.

Results and discussion

As shown in Fig. 1, all the XRD patterns of the as-synthesized MZ and MZP_x samples exhibit diffraction peaks in low angle region, indicating the mesostructural property. MZ shows three characteristic diffraction peaks corresponding to *d* spacings of 4.19, 2.40 and 2.09 nm (Fig. 1A), which can be indexed as (100), (110) and (200) of a hexagonal mesostructure with a lattice constant a_0 of 4.84 nm ($a_0=2d_{(100)}/\sqrt{3}$) [14, 15]. After the treatment with 0.1 M phosphoric acid solution, all the

three reflections are obviously strengthened (Fig. 1B) indicating a better long-range order, which should come from the complete condensation between P and Zr due to their stronger complexing ability [16]. Increasing the phosphoric acid concentration to 0.25-0.5 M (Fig. 1C and D) leads to similar XRD patterns to that of $MZP_{0.1}$. However, the intensity of (100) reflection decreases sharply once the phosphoric acid concentration reaches 0.76 M (Fig. 1E). Moreover, the disappearance of (110) and (200) reflections also indicate that the long-range order of $MZP_{0.76}$ is lowered. The (100) reflections of MZ and MZP_xs appear almost at the same position displaying that these samples have almost the same a_0s, which is a little different from the results of Ciesla et al. [15], who obtained enlarged a_0s after the H_3PO_4 treatment.

Fig. 2 gives the XRD patterns of the calcined MZP_x samples. After calcination at 723 K, no reflections can be observed for MZ sample showing that the mesostructure was destroyed. Whereas, calcination after the treatment with 0.1 M H_3PO_4 results in an obvious reflection in the low angle region indicating the presence of mesostructure in some extent. $MZP_{0.25}$ also exhibits such a reflection but with much higher intensity, which implies a better ordering. Further increasing the phosphoric acid concentration to 0.5-0.76 M, however, leads to gradually decreased reflections. Compared with the XRD patterns of Fig. 1, all the reflections of the calcined samples move to higher 2θ region inferring that lattice contractions have occurred during the calcinations, which agrees well with the previous reports [15, 17]. Fig. 2 also shows that the a_0 of the calcined samples increases with the increasing phosphoric acid concentration, which may be related to the fact that more P has been incorporated in the mesostructures when the phosphoric acid concentration increases [14]. The P in the framework of MZP_x reduces the lattice contraction effectively, thus larger a_0s are obtained.

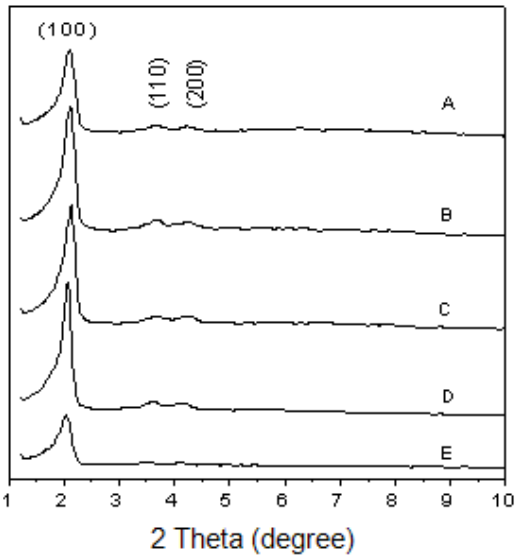

Fig. 1 XRD patterns of as-synthesized (A) MZ, (B) $MZP_{0.1}$, (C) $MZP_{0.25}$, (D) $MZP_{0.5}$ and (E) $MZP_{0.76}$.

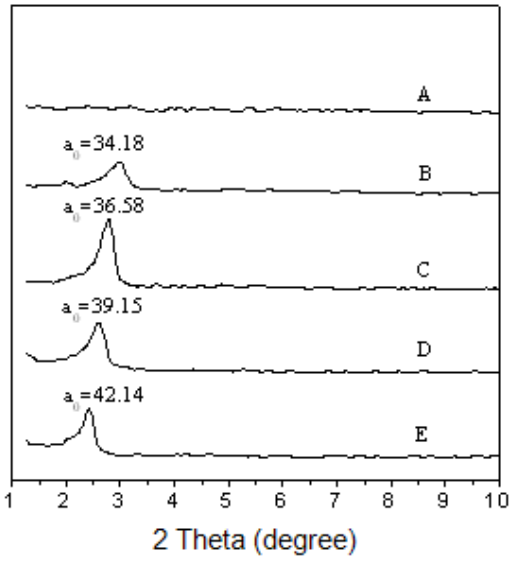

Fig. 2 XRD patterns of (A) MZ, (B) $MZP_{0.1}$, (C) $MZP_{0.25}$, (D) $MZP_{0.5}$ and (E) $MZP_{0.76}$ after calcination at 773 K (MZ) was calcined at 723 K).

FT-IR spectra of $MZP_{0.25}$ samples before and after calcination at 773 K are given in Fig. 3. For the as-synthesized sample (Fig. 3A), the broad bands at about 3500 and 1640 cm^{-1} stem from the absorbed water on the surface while the bands centered at 1000-1100 cm^{-1} should be attributed to the stretching vibration of phosphate groups [17-19]. The bands at 3000-2800 and 1477 cm^{-1} can be assigned respectively to the stretching and deformation vibrations of C-H of surfactant CTAB [18], which indicates the remaining of the structure-dircting agent. After calcination at 773 K (Fig. 3B), the vibration of phosphate groups merges into a broad one and the vibrations of C-H disappears. The latter showes that CTAB was removed completely. Take into accont that the calcined $MZP_{0.25}$ showed one reflection in low angle region (Fig. 2C), we speculate that porous material may be obtained. Fig. 4 depicts the N_2 isotherms of 773 K calcined MZP_xs. On the contrary to our speculation, $MZP_{0.25}$ exhibits an extremely low absorbed volume indicating a nonporous material (Fig. 4A), and the textual data showed that this sample has only a low BET specific surface area of 8

m^2/g. The results from N_2 adsorption method seem different from the XRD results. We prefer here the N_2 isotherm data since it is much precise in characterizing porous materials compared with the XRD method. Increasing the phosphoric acid concentration to 0.5 M, however, results in a type *I* isotherm showing that the 773 K calcined $MZP_{0.5}$ is a microporous material, as proved by its pore size of 0.6 nm and its BET specific surface area increase to 147 m^2/g. Interestingly, increasing the phosphoric acid concentration further to 0.76 M lowers the BET specific surface area down to 30 m^2/g.

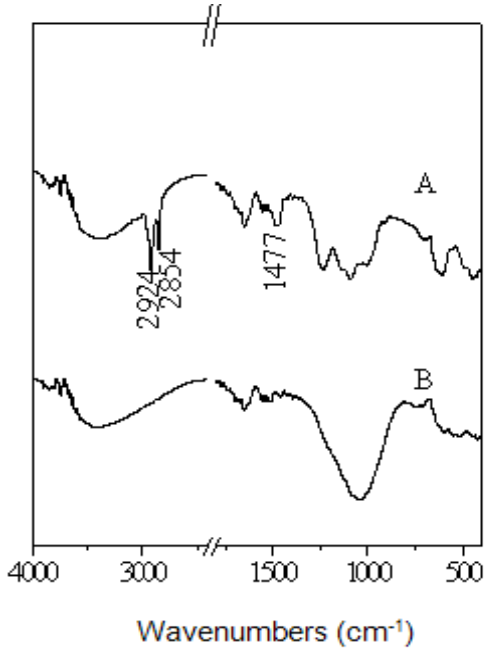

Fig. 3 FTIR spectra of $MZP_{0.25}$ (A) before and (B) after calcination at 773 K.

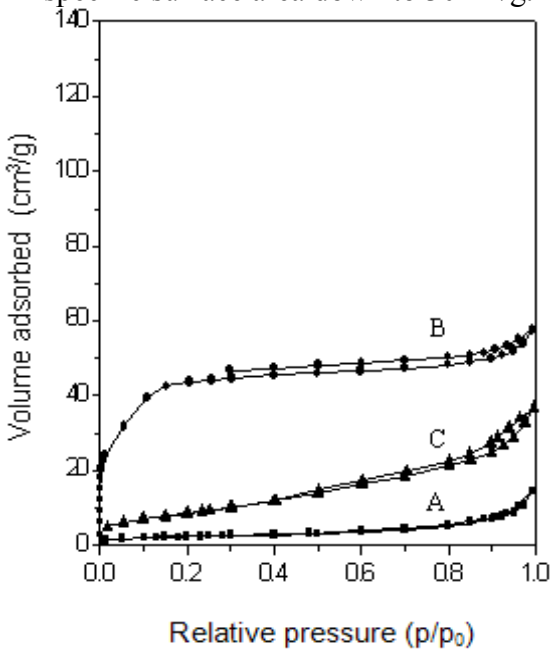

Fig. 4 N_2 adsorption isotherms of (A) $MZP_{0.25}$, (B) $MZP_{0.5}$ and (C) $MZP_{0.76}$ after calcination at 773 K.

Though porous materials can be obtained by chosing suitable phosphoric acid concentration, the BET specific surface area of the resulting MZP_x materials are still relatively low, which may be related to the larger framework density of MZP_x. So $AlCl_3$ solutions were used further to treat the MZP_x samples in order to introduce Al to the framework of MZP_x and such increase its BET specific surface area. The XRD patterns of the Zr-P-Al materials synthesized by treating MZP_x with the same amount of $AlCl_3$ solutions are showed in Fig. 5. All these as-synthesized samples exhibit reflections in low angle region indicating the existence of mesostructures, and no reflections in high angel region can be found suggesting the amorphous pore walls. The H_3PO_4 concentration affects the intensity of (100) reflections greatly. $MZP_{0.25}Al_{14}$ gives the most intensive (100) reflection together with a (110) one while only the (100) reflections with decreased intensities are observed for $MZP_{0.5}Al_{14}$ and $MZP_{0.76}Al_{14}$, indicating that the long-range of these mesostructures are degraded. Besides the varying of the intensities, the (100) reflection of MZP_xAl_{14} shifts gradually to the lower angle region implying the enlarging a_0s.

N_2 adsorption isotherms of 773 K calcined MZP_xAl_{14}s are given in Fig. 6. All the samples exhibit *type IV* isotherms, with strong uptakes of N_2 in a relative pressure (p/p_0) range of 0.2-0.4 due to capillary condensation predicting the formation of mesoporous structures. $MZP_{0.25}Al_{14}$ shows the largest absorbed volume and exhibits a BET specific surface area of 462 m^2/g. Increasing the phosphoric acid concentration further to 0.5-0.76 M decreases the BET specific surface area to 394 and 332 m^2/g, respectively. Whereas, the pore size of MZP_xAl_{14} increases from 2.9 nm for $MZP_{0.25}Al_{14}$ to 3.0 nm for $MZP_{0.5}Al_{14}$ and finally to 3.5 nm for $MZP_{0.76}Al_{14}$, which agree well with the XRD results. The N_2 adsorption results show that higher concentration of phosphoric acid will decrease the BET specific surface area though it can increase the pore size of MZP_xAl_{14}s. In order to obtain the highest BET specific surface area, the phosphoric acid concentration of 0.25 M was chosen to synthesize mesoporous MZP_xAl_y materials by adjusting the $AlCl_3$ amount.

We have reported that treating $MZP_{0.25}$ with different amount of $AlCl_3$ solution (y=0.7,1.8,7,14) led to reflections in the low angle region of $MZP_{0.25}Al_y$ on the XRD patterns, and that the (100) intensity of which changed hardly from $MZP_{0.25}Al_{0.7}$ to $MZP_{0.25}Al_7$ but increased suddenly for $MZP_{0.25}Al_{14}$ [14]. Increasing the y value further to 29, however, decreases the intensity a lot. After calcination at 773 K, The BET specific surface area of $MZP_{0.25}Al_y$ increased with the increasing y value, from 314, 393 and 453 m^2/g for $MZP_{0.25}Al_{0.7}$, $MZP_{0.25}Al_{1.8}$ and $MZP_{0.25}Al_7$, respectively, to 462 m^2/g for $MZP_{0.25}Al_{14}$. We also found that part of CTAB was removed during the $AlCl_3$ treatment, but no further works were carried out at that time. In the following part, thermal analysis method is used to characterize the removing of CTAB.

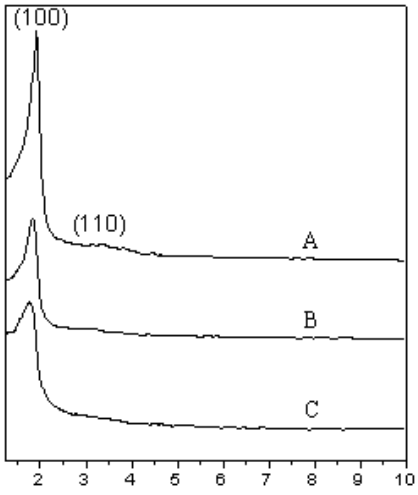

Fig. 5 XRD patterns of as-synthesized (A) $MZP_{0.25}Al_{14}$, (B) $MZP_{0.5}Al_{14}$ and (C) $MZP_{0.76}Al_{14}$.

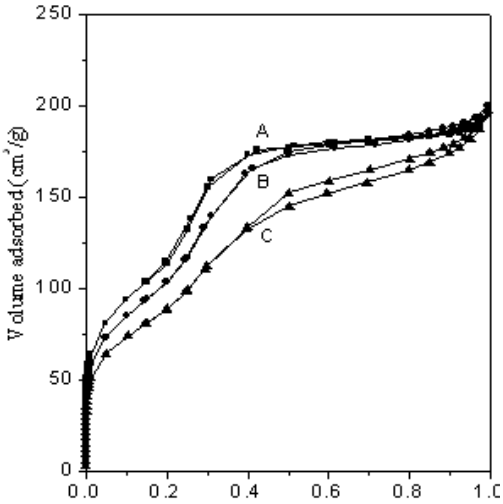

Fig. 6 N_2 adsorption isotherms of (A) $MZP_{0.25}Al_{14}$, (B) $MZP_{0.5}Al_{14}$ and (C) $MZP_{0.76}Al_{14}$ after calcination at 773

TGA profiles of $MZP_{0.25}$ and $MZP_{0.25}Al_{14}$ before and after calcination are depicted in Fig. 7, and corresponding DTA profiles are shown in Fig. 8. Figure 7A reveals three main steps of weight losses for $MZP_{0.25}$. The weight loss below 473 K is due to the desorption of water adsorbed physically and chemically [20], corresponding to the two overlapped endothermic peaks in the range 373-473 K in Fig. 8A. The other two weight losses occur in the range of 473-623 K and 623-923 K, respectively, associating with mainly two broad exothermic peaks in its DTA profile at the same stage (Fig. 8A), which may be related to the removal of CTAB. Figure 7B exhibits one weight loss in the range of 473-923 K and another in the range of 923-1173 K besides the one from water desorption. The former can be assigned to the removal of residual CTAB since no calcintion was performed and the latter to the decomposition of sulfate [21]. Compared with that of $MZP_{0.25}$, the DTA profile of as-synthesized $MZP_{0.25}Al_{14}$ shows no obvious exothermic peak (Fig. 8B) implying that only a small part of CTAB was remained in this sample, which agree well with the result from its TGA profile. After calciantion at 773 K, $MZP_{0.25}Al_{14}$ displays similar TGA profile to that of as-synthesized one, but a sharp exothermic peak centered at 1083 K shows up in the DTA profile (Fig. 8C), which is attributable to the occurrence of a crystalline transformation to tetragonal ZrO_2 since TGA curve does not show any weight loss at this stage. It has been reported that the crystalline transformation of H_3PO_4 treated mesoporous zirconia occurred in the range 873-1023 [22], and that the mesostructure would collapse down upon the crystallization into tetragonal ZrO_2 began [23]. As no crystallization can be observed for the as-synthesized $MZP_{0.25}Al_{14}$ in the whole range of temperature, we speculate that calcination decreases the thermal stabiltity of $MZP_{0.25}Al_{14}$ when it is heated again. Even though, the crystallization temperature of 1083 K for calcined $MZP_{0.25}Al_{14}$ is higher than those in literatures indicating a more thermally stable sample, as has been confirmed preceously [14].

Table 1 lists the values of the weight losses for $MZP_{0.25}$ and $MZP_{0.25}Al_{14}$ before and after calciantion. The weitht loss below 473 K for $MZP_{0.25}$ is about 3.5%, which is less than those of $MZP_{0.25}Al_{14}$ (more that 10% both). This may be caused by the fact that Al is a hydrophilic element,

thus more water is absorbed in $MZP_{0.25}Al_{14}$ than that in $MZP_{0.25}$. At the range of 473-923 K, $MZP_{0.25}$ shows a high weight loss of 34.5% while only 7.0 and 4.0% are observed for the $MZP_{0.25}Al_{14}$ before and after calcination, repectively. The former may be related to the decomposition of the larger amount of CTAB in $MZP_{0.25}$ as we will dicuss below. The weight loss of the as-synthesized $MZP_{0.25}Al_{14}$ is just 3% more than that of the calcined one, indicating that most of the surfactant has been removed during the $AlCl_3$ treatment, as inferrend from the FTIR spectra [14]. At the stage of 923-1173 K, $MZP_{0.25}Al_{14}$s both show similar weight loss due to the removal of residual S groups regardless of calcination or not. $MZP_{0.25}$ shows no weight loss at temperature higher than 923 K, however, the weight loss between 473-923 K is devided into two steps as we discussed above. Maybe CTAB can react with the S groups and the interaction shifts the removal of S groups towards the low temperature range compared with those of $MZP_{0.25}Al_{14}$s. The weight loss in the range of 473-623 K may be related to the oxidation of CTAB while that in the range of 623-923 K may be related to both the oxidation of CTAB and the removal of S groups. We confer that the weight loss from the removal of S groups for $MZP_{0.25}$ should be similar to that for $MZP_{0.25}Al_{14}$ (about 5%) since these samples posses similar S/Zr ratios [14]. Thus the weight loss from the oxidation of CTAB for $MZP_{0.25}$ is about 29.5%, which is about ten times of that in the as-synthesized $MZP_{0.25}Al_{14}$. That is, 90% of the CTAB have been removed during the $AlCl_3$ treatment, and porous materials may therefor be obtained for the as-synthesized sample.

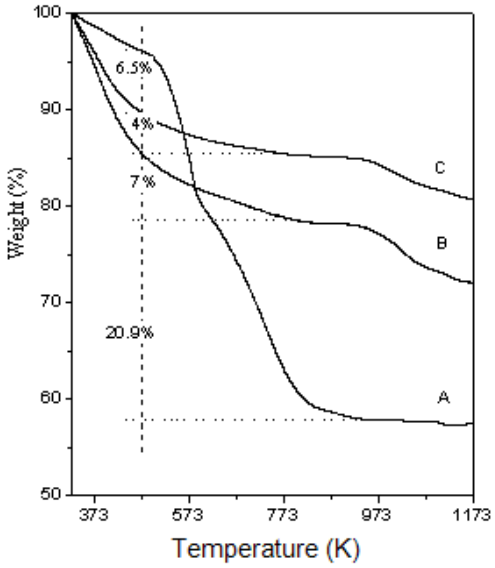

Fig. 7 TGA profiles of as-synthesized (A) $MZP_{0.25}$, (B) $MZP_{0.25}Al_{14}$ and (C) $MZP_{0.25}Al_{14}$ after calcination at 773 K.

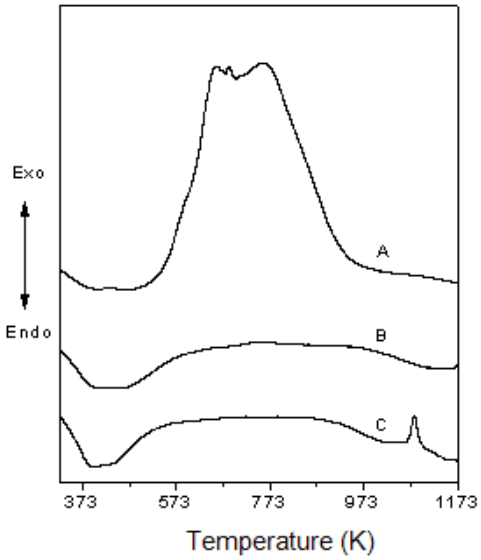

Fig. 8 DTA profiles of as-synthesized (A) $MZP_{0.25}$, (B) $MZP_{0.25}Al_{14}$ and (C) $MZP_{0.25}Al_{14}$ after calcination at 773 K.

Table 1 Weight losses (%) for $MZP_{0.25}$ and $MZP_{0.25}Al_{14}$ before and after calcination

Sample	323-473 (K)	473-923 (K)	923-1173 (K)
$MZP_{0.25}$	3.5	34.5	/
$MZP_{0.25}Al_{14}$	13.8	7	5.5
773 K calcined $MZP_{0.25}Al_{14}$	10.5	4	5.0

Fig. 9 gives the N_2 adsorption isotherms of as-synthesized $MZP_{0.25}Al_y$s, and corresponding textual data are listed in Table 2. The extremely low BET specific surface area of 32 m^2/g in Table 2 shows that $MZP_{0.25}$ is a non–porous material because of the existence of CTAB. However, $MZP_{0.25}Al_{0.7}$ shows an isotherm between type *I* and *IV* (Fig. 9A) indicating a porous material. The sample exhibits a pore volume of 0.23 cm^3/g and a pore size of 1.9 nm, and the BET specific surface area of which increases greatly to 477 m^2/g due to the removal of CTAB. Increasing the $AlCl_3 \cdot 6H_2O/MZP_{0.25}$ ratio to y=1.8 leads to a type *IV* isotherm (Fig. 9B), which exhibits a capillary condensation in a relative pressure (p/p_0) range of 0.1-0.2 implying a mesoporous material. Table 2 shows that this sample

possess a pore volume of 0.24 cm^3/g, a pore size of 2.2 nm and above all a high BET specific surface area of 521 m^2/g. Similar type *IV* isotherm is also obtained when y=14 (Fig. 9C), but the capillary condensation occurs at higher relative pressure indicating a bigger pore size [24]. Table 2 shows that this sample has a pore size of 2.4 nm as well as a pore volume of 0.33 cm^3/g. Strikingly, the BET specific surface area of as-synthesized $MZP_{0.25}Al_{14}$ increases sharply to 734 m^2/g. Table 2 also shows that the P/Zr and Al/Zr also increase when the $AlCl_3 \cdot 6H_2O/MZP_{0.25}$ ratio increases, and the highest ratios are obtained with y=14, where the highest BET specific surface area is resulted. Further increasing y to 29, whereas, results in decreased BET specific surface area as well as decreased pore volume though a mesoporous pore size of 2.6 nm can still be remained. According to our former works [14], a complex with layered structures in nanoscale dimension was formed for the Zr-P-Al materials. The pore walls of which contained layers of Al_2O_3, $(Zr\text{-}O)_2PO_2$ and ZrO_2 combining to each other from the inner to exterior. PO_2 works as the bonds in the three-layered structure units and is necessary for the Zr-P-Al materials.

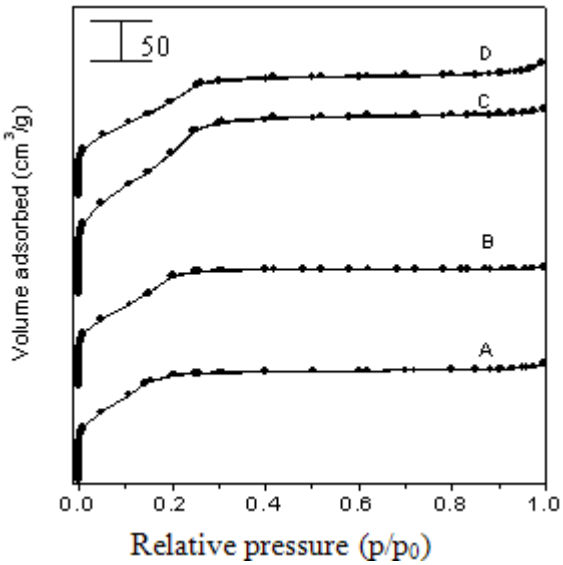

Fig. 9 N_2 adsorption isotherms of as-synthesized (A) $MZP_{0.25}Al_{0.7}$, (B) $MZP_{0.25}Al_{1.8}$,(C) $MZP_{0.25}Al_{14}$ and (D) $MZP_{0.25}Al_{29}$. The adsorbed volumes were offset by 60% for clarity.

Table 2 Textural data for the as-synthesized $MZP_{0.25}$ and $MZP_{0.25}Al_y$s

Sample	$d_{(100)}$ (nm)	BET specific surface area (m^2/g)	Pore volume (cm^3/g)	Pore size (nm)	P/Zr ratio	Al/Zr ratio
$MZP_{0.25}$	4.14	32	/	/	0.53	/
$MZP_{0.25}Al_{0.7}$	4.01	477	0.23	1.9	0.66	0.49
$MZP_{0.25}Al_{1.8}$	4.16	521	0.24	2.2	0.86	1.57
$MZP_{0.25}Al_{14}$	4.59	734	0.33	2.4	1.49	3.16
$MZP_{0.25}Al_{29}$	4.57	503	0.25	2.6	1.30	2.99

Conclusions

Treating the as-synthesized MZ sample with H_3PO_4 solutions leads to mesostructured MZP_x materials instead of the mesoporous ones, and further treatment with $AlCl_3$ solutions is necessary to obtain mesoporous MZP_xAl_y materials. The textual dada of MZP_xAl_y change with both the phosphoric acid concentration and the mass ratio of $AlCl_3 \cdot 6H_2O/MZP_x$. After calcination at 773 K, the BET specific surface area of MZP_xAl_{14} decreased while its pore size increased with the increasing H_3PO_4 concentration, but both increased for $MZP_{0.25}Al_y$ when the mass ratio of $AlCl_3 \cdot 6H_2O/MZP_{0.25}$ increased. Especially, $MZP_{0.25}Al_y$ (y>1.8) had already showed mesopores together with BET specific surface areas up to 734 m^2/g before calcination, which is very favorable both in industrial and environmental aspects.

References

[1] A. Taguchi, F. Schüth: Micropor. Mesopor. Mater. 77 (2005) 1-45.

[2] E. Iglesia, S.L. Soled, R.A. Fiato : J. Catal. 137 (1992) 212-224.

[3] A.Y. Khodakov, A. Griboval-Constant, R. Bechara, V.L. Zholobenko. J. Catal. 206 (2002) 230-241.

[4] A. Lewandowska, S. Monteverdi, M. Bettahar. M. Ziolek: J. Mol. Catal. A: Chem. 188 (2002) 85-95.

[5] C.T. Kresge, M.E. Leonowicz, W.J. Roth, J. C. Vartuli and J.S. Beck: Nature. 359 (1992) 710-712

[6] J.S. Beck, J.C. Vartuli, W.J. Roth, M.E. Leonowicz, C.T. Kresge, K.D. Schmitt, C.T.W. Chu, D.H. Olson, E.W. Sheppard, S.B. McCullen, J.B. Higgins. J. L. Schlenker: J. Am. Chem. Soc. 114 (1992) 10834-11843.

[7] Z.S. Chao. E. Ruckenstein: Langmuir. 18 (2002) 8535-8545.

[8] G.K. Chuah, S.H. Liu, S. Jaenicke, J. Li: Micropor. Mesopor. Mater. 39 (2000) 381-392.

[9] J.N. Kondo, Y. Takahara, D.L. Lu , K. Domen: Chem. Mater. 13 (2001) 1200-1206.

[10] F. Vaudry, S. Khodabandeh, M.E. Davis: Chem. Mater. 8 (1996) 1451-1464.

[11] J. Blanchard, F. Schüch, P. Trens, M. Hudson: Micropor. Mesopor. Mater. 39 (2000) 163-170.

[12] F. Schüch: Chem. Mater. 13 (2001) 3184-3195.

[13] Z.Y. Liu, Y. Qi, Y. Zhang, L.H. Qu, S.Y Sang, Z.M. Liu: Chin. J. Catal. 26 (2005) 475-479.

[14] Z.Y. Liu, Y.X. Wei, Y. Qi, X.B. Liu, Y.F. Zhao, Z.M. Liu: Micropor. Mesopor. Mater. 91 (2006) 225-232.

[15] U. Ciesla, S. Schacht, G.D. Stucky, K.K. Unger, F. Schüth: Angew, Chem. Int. Ed. Engl. 35 (1996) 541-543.

[16] J. Livage, M. Henry, C. Sanchez: Prog. Solid State Chem. 18 (1988) 259-341.

[17] W. Liu, Z.X. Song, T. Ikegawa, H. Nishiguchi, T. Ishihara, Y. Takita, Mater. Lett. 58 (2004) 3328-3331.

[18] F. Kleitz, S.J. Thomson, Z. Liu, O. Terasaki and F. Schüch: Stud. Surf. Sci. Catal. 146 (2003) 221-225.

[19] H.R. Chen, J.L. Shi, W.H. Zhang, D.S. Yan J. Inorg. Mater: 15 (2000) 1123-1126.

[20] T. Sreethawong, S. Ngamsinlapasathian, Y. Suzuki , S. Yoshikawa: J. Mol. Catal. A: Chem. 235 (2005) 1-11.

[21] C.L. Chen, T. Li, S. Cheng, H.P. Lin, C.J. Bhongale, C.Y. Mou: Micropor. Mesopor. Mater. 50 (2001) 201-208.

[22] U. Ciesla, M. Fröba, G. Stucky, F. Schüth: Chem. Mater. 11 (1999) 227-234.

[23] U. Ciesla, G. Stucky, F.F. Schüth: Stud. Surf. Sci. Catal. 117 (1998) 527-534.

[24] X.B. Liu, F.X. Chang, L. Xu, Y. Yang, P. Tian, L.L. Qu, Z.M. Liu: Micropor. Mesopor. Mater. 79 (2005) 269-273.

Applications of Engineering Materials
10.4028/www.scientific.net/AMR.287-290

Synthesis of Mesoporous Zr-P-Al Materials with High BET Specific Surface Area without Calcination

10.4028/www.scientific.net/AMR.287-290.2094